



HAL
open science

Neural epidermal growth factor-like 1 protein (NELL-1) associated membranous nephropathy

Sanjeev Sethi, Hanna Debiec, Benjamin Madden, M Cristine Charlesworth,
Johann Morelle, Louann Gross, Aishwarya Ravindran, David Buob, Michel
Jadoul, Fernando Fervenza, et al.

► To cite this version:

Sanjeev Sethi, Hanna Debiec, Benjamin Madden, M Cristine Charlesworth, Johann Morelle, et al..
Neural epidermal growth factor-like 1 protein (NELL-1) associated membranous nephropathy. *Kidney
International*, 2020, 97 (1), pp.163-174. 10.1016/j.kint.2019.09.014 . hal-02433666

HAL Id: hal-02433666

<https://hal.sorbonne-universite.fr/hal-02433666>

Submitted on 9 Jan 2020

HAL is a multi-disciplinary open access archive for the deposit and dissemination of scientific research documents, whether they are published or not. The documents may come from teaching and research institutions in France or abroad, or from public or private research centers.

L'archive ouverte pluridisciplinaire **HAL**, est destinée au dépôt et à la diffusion de documents scientifiques de niveau recherche, publiés ou non, émanant des établissements d'enseignement et de recherche français ou étrangers, des laboratoires publics ou privés.

Neural epidermal growth factor-like 1 protein (NELL-1) associated membranous nephropathy



see commentary on page 29
OPEN

Sanjeev Sethi¹, Hanna Debiec^{2,3,10}, Benjamin Madden^{4,10}, M. Cristine Charlesworth⁴, Johann Morelle^{5,6}, LouAnn Gross¹, Aishwarya Ravindran¹, David Buob^{2,3,7}, Michel Jadoul^{5,6}, Fernando C. Fervenza^{8,11} and Pierre Ronco^{2,3,9,11}

¹Department of Laboratory Medicine and Pathology, Mayo Clinic, Rochester, Minnesota, USA; ²Sorbonne Université, Université Pierre et Marie Curie Paris 06, Paris, France; ³Institut National de la Santé et de la Recherche Médicale, Unité Mixte de Recherche S 1155, Paris, France; ⁴Medical Genome Facility, Proteomics Core, Mayo Clinic, Rochester, Minnesota, USA; ⁵Division of Nephrology, Cliniques universitaires Saint-Luc, Brussels, Belgium; ⁶Institut de Recherche Expérimentale et Clinique, UCLouvain, Brussels, Belgium; ⁷Department of Pathology, Tenon Hospital, Paris, France; ⁸Division of Nephrology and Hypertension, Mayo Clinic, Rochester, Minnesota, USA; and ⁹Hôpital de Jour—Nephrology, Assistance Publique-Hôpitaux de Paris, Paris, France

Membranous nephropathy is characterized by deposition of immune complexes along the glomerular basement membrane. PLA2R and THSD7A are target antigens in 70% and 1-5% of primary membranous nephropathy cases, respectively. In the remaining cases, the target antigen is unknown. Here, laser microdissection of glomeruli followed by mass spectrometry was used to identify novel antigen(s) in PLA2R-negative membranous nephropathy. An initial pilot mass spectrometry study in 35 cases of PLA2R-negative membranous nephropathy showed high spectral counts for neural tissue encoding protein with EGF-like repeats, NELL-1, in six cases. Mass spectrometry failed to detect NELL-1 in 23 PLA2R-associated membranous nephropathy and 88 controls. NELL-1 was localized by immunohistochemistry, which showed bright granular glomerular basement membrane staining for NELL-1 in all six cases. Next, an additional 23 NELL-1 positive cases of membranous nephropathy were identified by immunohistochemistry in a discovery cohort of 91 PLA2R-negative membranous nephropathy cases, 14 were confirmed by mass spectrometry. Thus, 29 of 126 PLA2R-negative cases were positive for NELL-1. PLA2R-associated membranous nephropathy and controls stained negative for NELL-1. We then identified five NELL-1 positive cases of membranous nephropathy out of 84 PLA2R and THSD7A-negative cases in two validation cohorts from France and Belgium. By confocal microscopy, both IgG and NELL-1 colocalized to the glomerular basement membrane. Western blot analysis showed reactivity to NELL-1 in five available sera, but no reactivity in control sera. Clinical and biopsy

findings of NELL-1 positive membranous nephropathy showed features of primary membranous nephropathy. Thus, a subset of membranous nephropathy is associated with accumulation and co-localization of NELL-1 and IgG along the glomerular basement membrane, and with anti-NELL-1 antibodies in the serum. Hence, NELL-1 defines a distinct type of primary membranous nephropathy.

Kidney International (2020) **97**, 163–174; <https://doi.org/10.1016/j.kint.2019.09.014>

KEYWORDS: mass spectrometry; membranous nephropathy; NELL-1
Copyright © 2019, International Society of Nephrology. Published by Elsevier Inc. This is an open access article under the CC BY-NC-ND license (<http://creativecommons.org/licenses/by-nc-nd/4.0/>).

Membranous nephropathy (MN) results from antibodies targeting an antigen in the glomerular basement membrane (GBM).^{1–3} The target antigen has been identified as M-type phospholipase A2 receptor (PLA2R) and thrombospondin type-1 domain-containing 7A (THSD7A) in approximately 70% and 1% to 5% of primary MN, respectively.^{4–6} The target antigen(s) in the remaining PLA2R- and THSD7A-negative primary MN has remained elusive. The aim of this study was to identify an antigen(s) in the remaining primary MN.

We used the novel methodology of laser microdissection and mass spectrometry to identify the major proteins in MN followed by immunostaining to localize and characterize the unique proteins. In the first step, we established that PLA2R antigen can be detected in PLA2R-positive MN. In the second step, we determined whether we could detect unique protein(s) with similar expression to PLA2R in a subset of PLA2R-negative MN.

RESULTS

Patient and biopsy collection

We initially selected 35 cases (pilot cohort) of PLA2R-negative MN on kidney biopsy for analysis by tandem mass spectrometry (MS/MS), and detected the unique protein, NELL-1,

Correspondence: Sanjeev Sethi, Department of Laboratory Medicine and Pathology, 200 1st Street SW, Mayo Clinic, Rochester, Minnesota 55905, USA. E-mail: sethi.sanjeev@mayo.edu

¹⁰HD and BM contributed equally to this work and are co-second authors.

¹¹FCF and PR contributed equally to this work.

Received 28 August 2019; revised 10 September 2019; accepted 12 September 2019; published online 7 October 2019

a neural tissue encoding protein with epidermal growth factor (EGF)-like repeats in 6 cases. We then analyzed the 35 cases of the pilot MS/MS and 91 additional PLA2R-negative MN cases by immunohistochemistry (IHC) for NELL-1 staining (discovery cohort). IHC confirmed the 6 positive NELL-1 cases of the pilot cohort and detected an additional 23 cases of NELL-1, bringing the total of NELL-1-positive cases to 29 (Figure 1). We performed MS/MS in 14 available samples of the 23 additional IHC NELL-1-positive cases from the discovery cohort to confirm the presence of NELL-1.

MS/MS detection of NELL-1 in PLA2R-negative biopsies

Glomeruli were dissected (Figure 2a) and MS/MS studies from 35 PLA2R-negative MN cases (pilot cohort) detected the unique protein NELL-1 in 6 cases of the pilot cohort (Figure 2b). The average total spectral count for NELL-1 was 63.1 (SD \pm 21.6) per case and is comparable to total spectral counts of PLA2R (86.1, SD \pm 27.5) and Exostosin-1 (EXT1)/Exostosin-2 (EXT2) (EXT1: 65.3, SD \pm 34.6; EXT2: 83.4, SD \pm 38.4) in PLA2R-associated and EXT1/EXT2-associated MN, respectively.⁷ All controls including PLA2R-associated MN cases were negative for NELL-1. MS/MS showed baseline spectral counts of PLA2R (average: 9.6, SD \pm 8.6) in NELL-1-associated MN. The spectral counts of NELL-1 in the 6 cases, along with representative sequence coverage map of NELL-1 from 1 case are shown in Figure 2b and c. We subsequently performed MS/MS in 14 of 23 cases of the discovery cohort cases that were positive for NELL-1 by IHC. All cases showed

similar high spectral counts of NELL-1 (Figure 2d). An example of MS/MS spectra match to a sequence from NELL-1 is shown in Supplementary Figure S1.

All 4 classes of Igs were detected in NELL-1-associated MN: IgG1 was the most abundant Ig (average: 63.6, SD \pm 13.1), followed by IgG3 (average: 53.2, SD \pm 19.6), IgG2 (average: 50.6, SD \pm 23.9), and IgG4 (average: 35.5, SD \pm 18.2).

IHC staining for NELL-1 in PLA2R-negative biopsies

We performed IHC staining for NELL-1 in 126 cases of PLA2R-negative MN from the pilot and discovery cohorts. Twenty-nine cases (23.0%) were positive for NELL-1 (6 in the pilot and 23 in the discovery cohort). All 29 positive cases showed bright (2–3+/3) granular staining for NELL-1 along the GBM. Importantly, there was no significant mesangial staining. NELL-1 staining in 6 cases is shown in Figure 3a. Segmental granular capillary wall staining for NELL-1 was seen in 6 cases (20.6%). Review of electron microscopy confirmed the segmental subepithelial deposits in all 6 cases (Supplementary Figure S2). There was no staining along the Bowman's capsule, tubular basement membranes, or in vessel walls. The positive NELL-1 granular staining mirrored the granular IgG along the GBM seen in each case. All control cases were negative for NELL-1. Representative negative staining for NELL-1 in PLA2R-associated MN, focal segmental glomerulosclerosis, IgA nephropathy, and diabetes is shown in Figure 3b. Representative NELL-1 staining in the

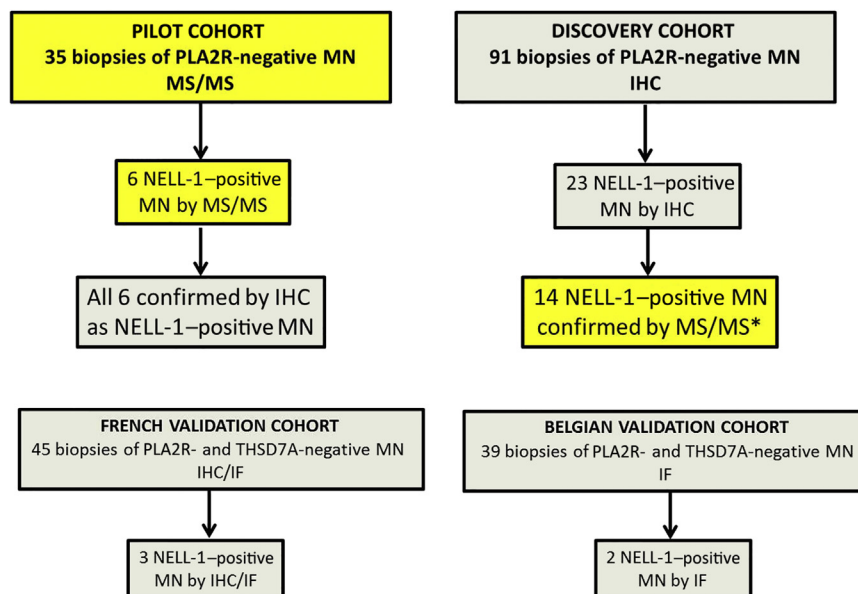


Figure 1 | Flowchart of the pilot, discovery, and validation cohorts. Initial pilot studies were done by mass spectrometry (MS) studies using 35 M-type phospholipase A2 receptor (PLA2R)-negative membranous nephropathy (MN) cases. We detected neural epidermal growth factor-like 1 protein (NELL-1) in 6 cases, which was then confirmed by immunohistochemistry (IHC). We then studied a large number ($n = 91$) of PLA2R-negative MN cases for expression of NELL-1 by IHC (discovery cohort). This yielded an additional 23 NELL-1-positive MN cases. We then confirmed the positive IHC NELL-1 staining in 14 cases by MS/MS. Two validation cohorts were studied. The first (French) validation cohort included 45 cases of PLA2R- and thrombospondin type-1 domain-containing 7A (THSD7A)-negative cases, of which 3 were positive for NELL-1 on IHC/immunofluorescence (IF). The second (Belgian) validation cohort included 39 cases of PLA2R- and THSD7A-negative cases, of which 2 were positive for NELL-1 on IF studies. Gray boxes indicate IHC or IF studies, and yellow boxes indicate MS/MS studies. *In the remaining 9 cases, we did not perform MS/MS.

remaining NELL-1-positive MN is also shown in the [Supplementary Figure S3](#).

Validation cohorts

Five of 90 cases (5.9%) of PLA2R- and THSD7A-negative MN were positive for NELL-1 staining in the validation cohorts.

French cohort. Three of 45 cases (6.7%) were positive for NELL-1 staining. The first positive case (patient 30) was detected at the Mayo Clinic and the remaining 2 cases (patients 31 and 32) at Tenon Hospital. Both IHC and immunofluorescence (IF) studies for NELL-1 were done in the first case (patient 30), while IF studies were done for NELL-1 detection in the other 2 cases (patients 31 and 32) ([Figure 3c](#)).

Belgian cohort. Two of 39 cases (5.1%) (patients 33 and 34) were positive for NELL-1 staining by IF staining ([Figure 3d](#)). Those cases were recruited at Cliniques universitaires Saint-Luc in Brussels and detected at Tenon Hospital.

Confocal microscopy

We performed confocal IF microscopy to show that the NELL-1 and IgG colocalize along the GBM ([Figure 4](#)). Superimposition of the 2 signals (yellow, [Figure 4c](#) and [f](#)) and laser quantitative analysis ([Figure 4g](#)) confirm the colocalization of NELL-1 and IgG, further corroborating that the subepithelial deposits contain both NELL-1 and IgG. A second case is shown in [Supplementary Figure S4](#).

Western blot analysis

Western blot analyses were performed using recombinant human NELL-1 to determine the presence of circulating anti-NELL-1 antibodies in the serum of 5 patients—4 patients from the validation cohort and 1 from the discovery cohort. All 5 patients showed reactivity against NELL-1 under nonreducing conditions (patients are labeled as MN in [Table 1](#)); NELL-1 was detected as a 280-kDa homodimer and a 420-kDa homotrimer. Furthermore, sera were available at different points in patient MN2. The MN2 sera were tested both prior to and during follow-up ([Figure 5a](#)). Sera from patients with PLA2R-associated MN, minimal change disease, and IgA nephropathy did not show any reactivity against NELL-1. There was no reactivity under reducing conditions where NELL-1 resolves as monomeric bands of about 130 kDa, suggesting that NELL-1 autoantibody recognizes conformation-dependent epitopes.

Finally, we also characterized the NELL-1 autoantibodies and showed that the predominant IgG subclass is IgG1 in patients MN1 and MN3, and IgG2 and IgG4 were also present along with IgG1 in patient MN2 ([Figure 5b](#)).

Clinical and kidney biopsy findings of NELL-1-associated MN

We identified 29 cases of NELL-1-associated MN from the pilot and discovery cohorts (patients 1–29). There were 15 male patients (51.7%) and 14 female patients (48.3%). The mean age at presentation was 63.1 ± 10.4 years. The mean serum creatinine and proteinuria at presentation was 1.7 ± 1.4 mg/dl (SD) and 6.9 ± 3.4 g/24 h, respectively. Twenty-four-hour urinary

protein was not done in 7 patients. With the exception of 1 patient with positive antinuclear antibody titers, serologies including hepatitis were negative.

The kidney biopsy of all cases of NELL-1-associated MN showed the characteristic findings of thickened GBM on light microscopy, bright IgG and complement component 3 (C3) staining along the capillary wall on IF microscopy, and subepithelial deposits on electron microscopy. Overall, an average of 20.6 ± 13.7 glomeruli were present, of which 3.2 ± 4.6 were globally sclerosed. IF microscopy showed bright staining for IgG (2–3+/3) and C3 (1–3+/3) in all cases. Only 1 case showed 1+ IgA, and 2 cases showed 1+ C1q. The remaining cases were negative for IgA, IgM, and C1q. All cases showed staining for kappa (2–3+/3) and lambda (2–3+/3) light chains. IF staining for PLA2R was negative in all cases. Electron microscopy showed subepithelial deposits in all cases, and in 6 cases, the subepithelial deposits were present in a segmental manner involving some but not all the capillary loops. Subendothelial and mesangial deposits were not present. Tubuloreticular inclusions were not present.

The 3 positive NELL-1 cases of the French validation cohort were also older patients—2 male and 1 female. Interestingly, one (patient 30) had lung cancer (epidermoid type), another (patient 31) had metastatic pancreatic carcinoma, and the third (patient 32) had metastatic breast cancer. In all 3 patients of that cohort, cancer was discovered at the time of, or a few months after, the diagnosis of MN. One (patient 33) of the 2 positive NELL-1 cases of the Belgian validation cohort was young woman while the other (patient 34) was an older male patient. Interestingly, patient 34 developed infiltrating urothelial carcinoma 8 months after diagnosis of MN. The clinical and pathology findings are shown in [Table 1](#).

DISCUSSION

MN is the most common cause of nephrotic syndrome in Caucasian adults. It is caused by autoantibodies against target antigens in the GBM and subsequent formation of antigen-antibody complexes. Based on the identification of the target antigen, MN is also classified as PLA2R-positive (70%), THSD7A-positive (1%–5%), and PLA2R/THSD7A-double negative MN. In the PLA2R/THSD7A-double negative cases, the target antigen(s) remain elusive. We have recently identified 2 novel proteins, EXT1 and EXT2, in patients with secondary MN associated with autoimmune disease.⁷ We used a combination of laser microdissection, MS/MS, and IHC techniques to identify EXT1 and EXT2. We reasoned that we could identify the elusive antigen(s) of the remaining 20% to 30% of primary PLA2R- and THSD7A-negative MN cases using the same methodology.

Laser microdissection combined with MS/MS allows for the identification of a large number of proteins along with estimates of their relative abundance using total spectral counts. In this study, we were able to identify 1500 to 2000 glomerular proteins per case, most of which are housekeeping proteins, many with low total spectral counts. Previously, we

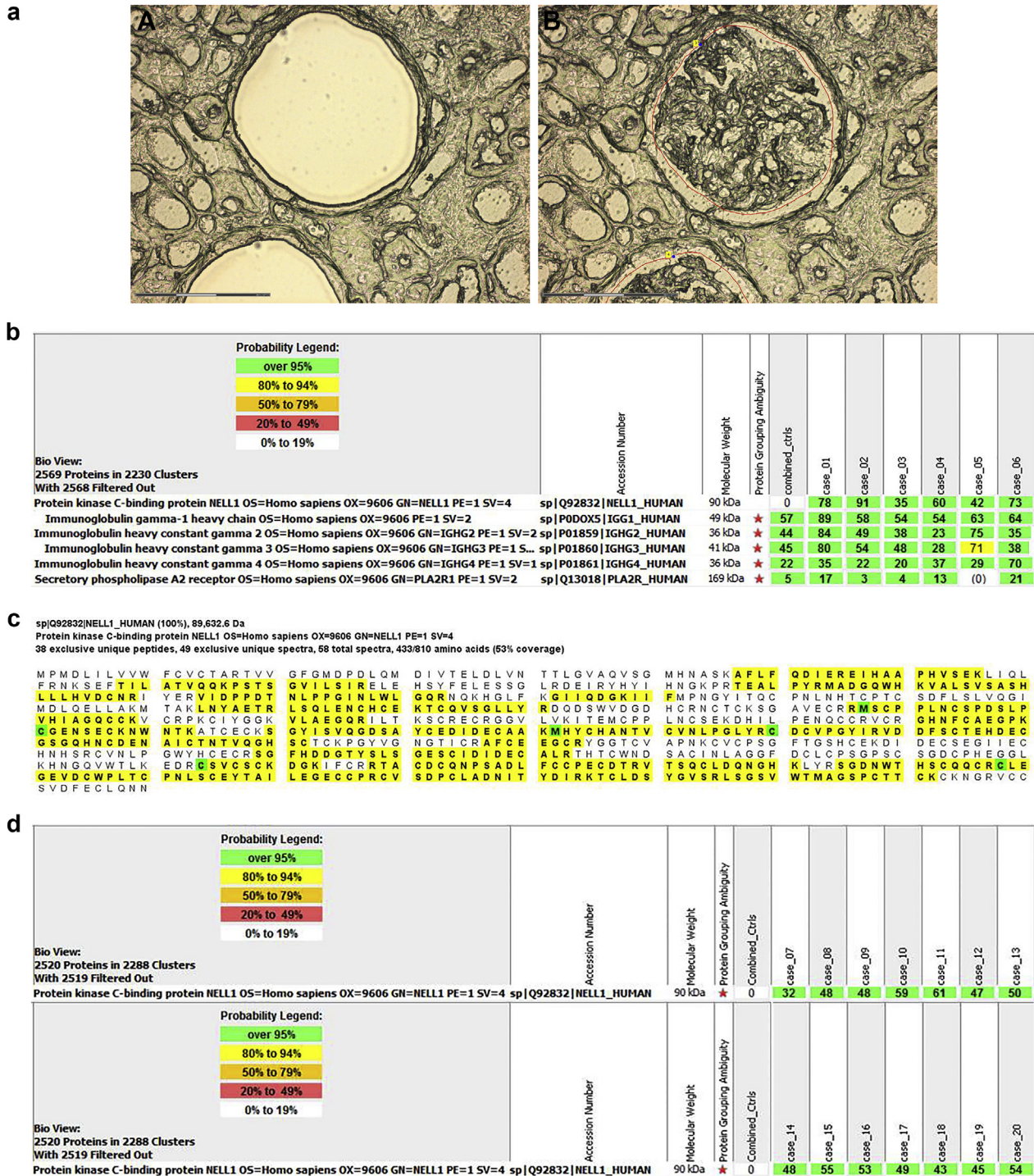


Figure 2 | Proteomic identification of neural epidermal growth factor-like 1 protein (NELL-1) in M-type phospholipase A2 receptor (PLA2R)-negative membranous nephropathy cases. Glomeruli were microdissected and analyzed using mass spectrometry as described in the Methods. (a) A glomerulus marked for dissection and vacant space on slide following microdissection are shown. Bars = 150 μm. (b) The table shows high spectral counts of NELL-1 in 6 cases of PLA2R-negative membranous nephropathy. Numbers in green boxes represent spectral counts of tandem mass spectrometry matches to a respective protein. All 6 cases show large total spectral counts for NELL-1 and Igs; baseline spectral counts of PLA2R were detected in 5 of 6 cases. For comparison, the average total spectral counts from 6 control cases (ctrls) (day 0 protocol transplant biopsies) are also shown. (c) The representative sequence coverage map of NELL-1 from 1 case. Amino acids highlighted in bold letters over yellow background are the amino acids detected. Note the extensive coverage. Green highlighted boxes indicated amino acids with artifactual chemical modification induced by mass spectrometry, such as oxidation of methionine. (d) The table shows the detection of NELL-1 on tandem mass spectrometry in an additional 14 NELL-1-associated membranous nephropathy cases of the discovery cohort. OS, species; OX, taxonomy identifier; PE, protein evidence score; SV, sequence version. To optimize viewing of this image, please see the online version of this article at www.kidney-international.org.

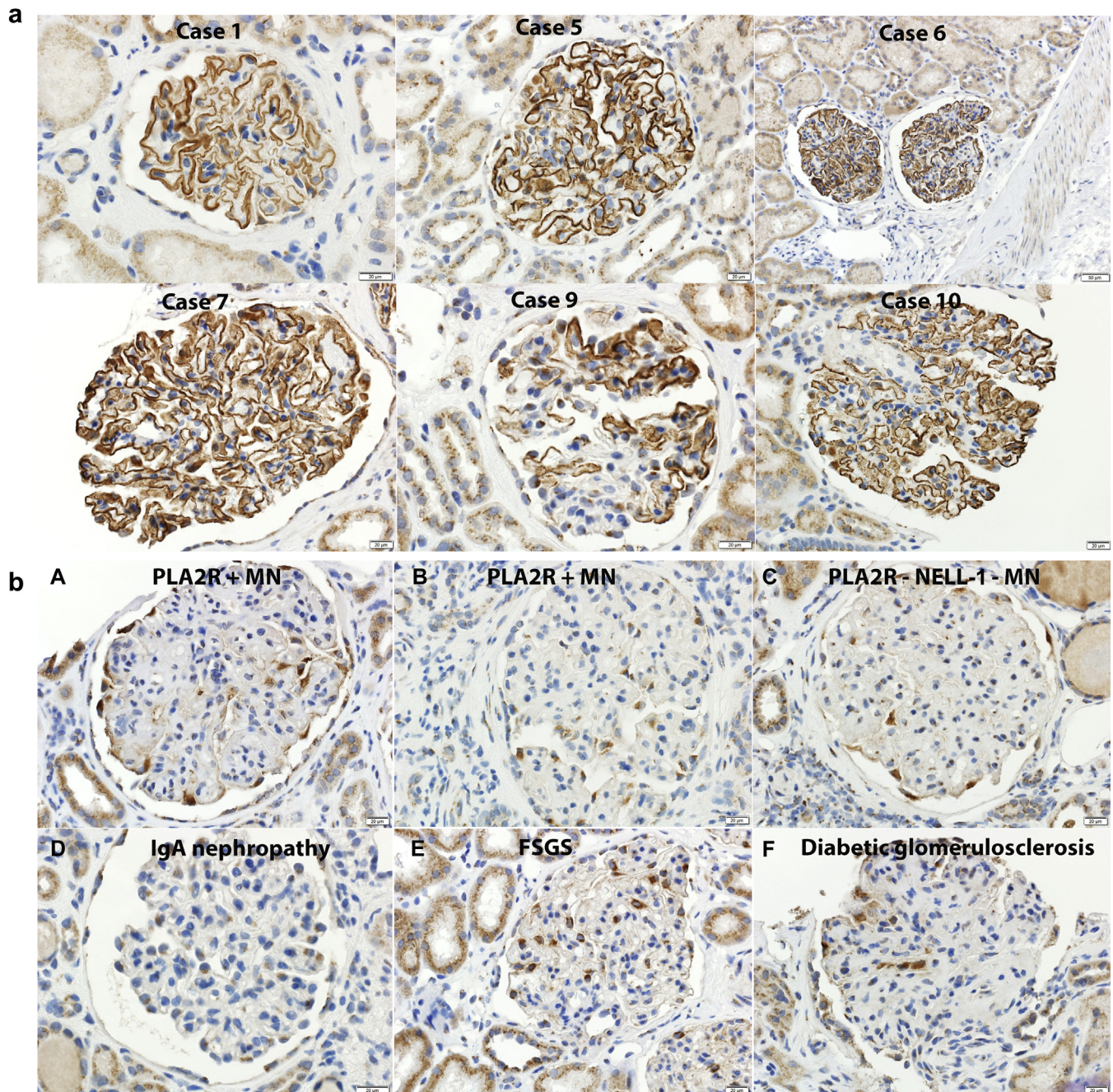


Figure 3 | Immunohistochemical (IHC) stain for neural epidermal growth factor-like 1 protein (NELL-1) in NELL-1-associated membranous nephropathy (MN), M-type phospholipase A2 receptor (PLA2R)-associated MN, and control cases. (a) The bright granular capillary wall staining for NELL-1 along the glomerular basement membranes in 6 cases of NELL-1-associated MN are shown. Note the segmental capillary wall staining in case 9. **(b)** The negative NELL-1 staining in control cases are shown. There was no capillary wall staining for NELL-1 in **(A,B)** 2 cases of PLA2R-associated MN, **(C)** an additional case that was PLA2R-negative but also NELL-1-negative, **(D)** IgA nephropathy, **(E)** focal segmental glomerulosclerosis (FSGS), and **(F)** diabetic glomerulosclerosis. Note very weak podocyte staining for NELL-1 but negative capillary wall staining. (Continued)

found that PLA2R was among the most abundant protein in PLA2R-associated MN compared with the housekeeping proteins.⁷ Here, we detected a novel protein, NELL-1, in glomeruli dissected from PLA2R-negative MN. The NELL-1 spectral counts were among the highest and were comparable to the Igs, complement proteins, and basement membrane structural proteins and were similar to the counts of PLA2R

and EXT1/EXT2 present in PLA2R- and EXT1/EXT2-associated MN. The high NELL-1 spectral count was also validated by the extensive sequence coverage found for the NELL-1 protein. There were 0 NELL-1 spectral counts in PLA2R-positive MN and control cases.

IHC confirmed MS/MS data and revealed bright granular capillary wall NELL-1 staining that was evenly spread

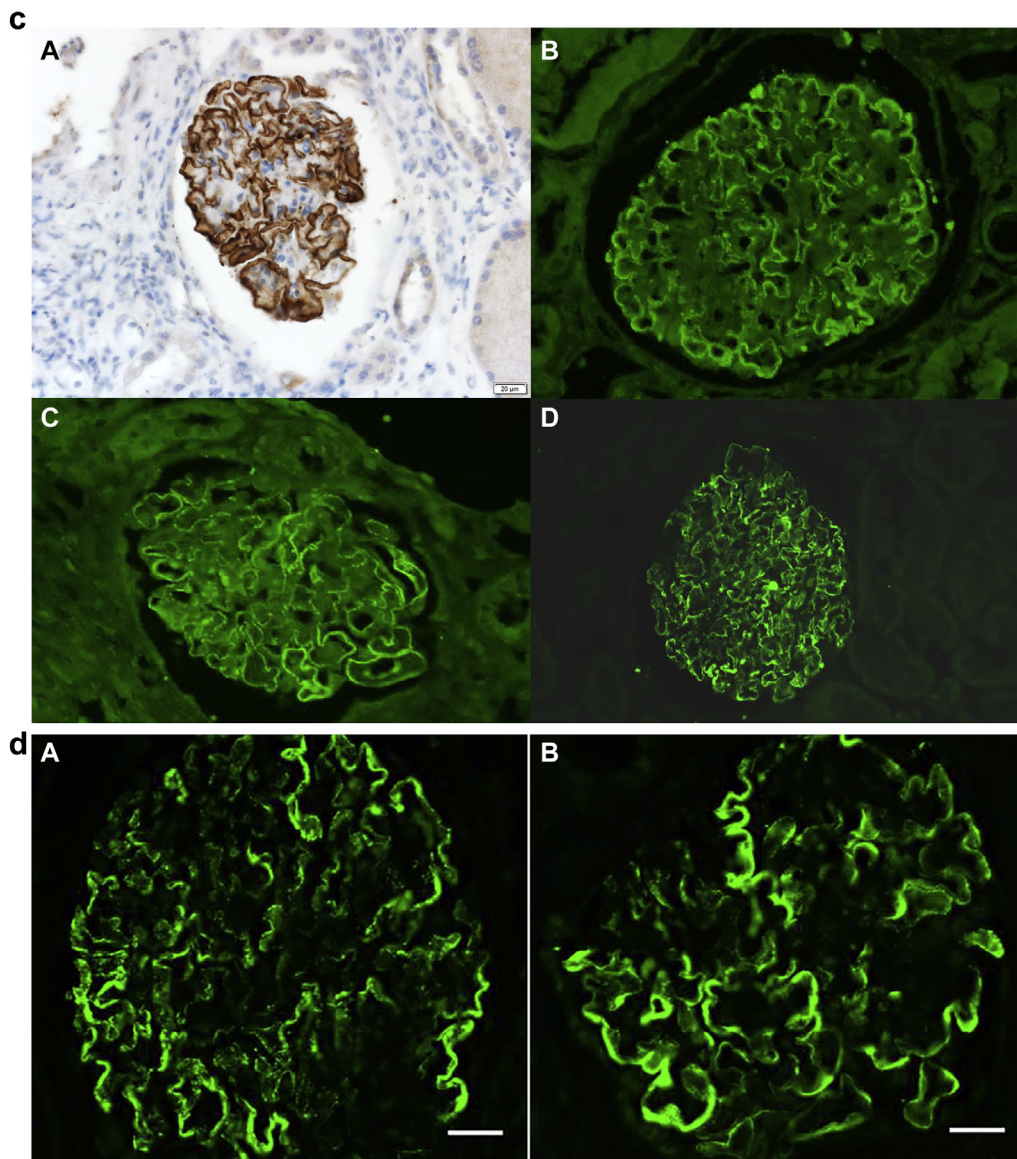


Figure 3 | (Continued) (c) Immunofluorescence (IF) and IHC show bright capillary wall staining for NELL-1 of 3 cases of the French validation cohort. (A,B) Case 1 (patient 30) was stained by both IHC and IF, and (C,D) the remaining 2 cases (patients 31 and 32) were stained with IF only. (d) IF shows capillary wall staining for NELL-1 of (A,B) 2 cases of the Belgian validation cohort. Bars = 20 μm. To optimize viewing of this image, please see the online version of this article at www.kidney-international.org.

throughout the thickened GBM and mirrored the IgG staining. There was 100% concordance of MS/MS and IHC; that is, all NELL-1–positive MN cases detected on MS/MS (pilot cohort) were positive on IHC and all NELL-1–positive MN cases detected on IHC (discovery cohort) were also positive for NELL-1 on MS/MS. Interestingly, there was segmental positive IHC staining for NELL-1 in a few cases; electron microscopy in these cases also showed segmental subepithelial deposits. The uniformity of NELL-1 staining along the GBM and correlation with the subepithelial deposits suggests that this protein is shed from the podocytes rather than representing circulating entrapped antigens or immune complexes. It is unlikely that NELL-1 is shed from mesangial cells or endothelial cells because there was no mesangial or

subendothelial staining in the NELL-1–positive MN. Furthermore, IF confocal microscopy studies showed that both NELL-1 and IgG colocalized to the GBM, indicating that NELL-1 is the likely target antigen for the IgG. This was further confirmed by demonstration of circulating antibodies to NELL-1 in the sera of 5 patients. In 1 patient (MN2) in whom sera was available at different time points, reactivity to NELL-1 had decreased at the time of treatment with anti-CD20 agent rituximab and completely disappeared thereafter although proteinuria persisted. This suggests that the patient was undergoing spontaneous immunological remission but the lack of clinical remission is in keeping with results seen in PLA2R-associated MN where proteinuria lags behind depletion of PLA2R antibodies.⁸ Our suggestion that

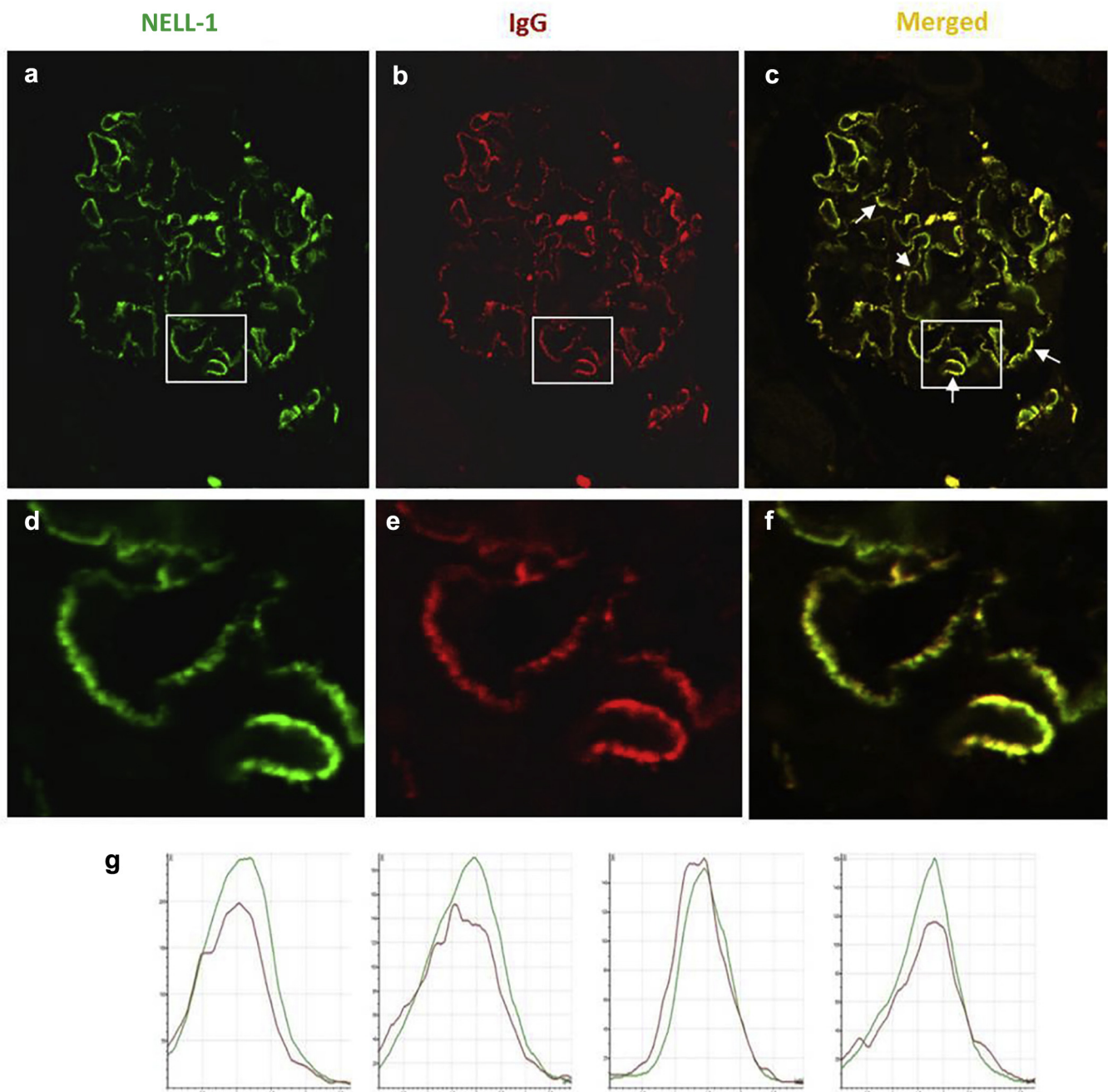


Figure 4 | Detection of neural epidermal growth factor-like 1 protein (NELL-1) and IgG in glomerular-immune deposits in NELL-1-associated membranous nephropathy cases by confocal immunofluorescence microscopy analysis. Glomeruli double-labeled with (a) anti-NELL-1 (green) and (b) anti-human IgG (red); (c) the merged image is shown. (d–f) These images are enlarged images of the boxed areas in a, b, and c, respectively. (g) The graphs show quantitative analysis of the fluorescence recorded across sections of a representative capillary loop (indicated by arrows in c). Note the superimposition of the 2 signals, which indicates that subepithelial immune deposits contain NELL-1 (green) and IgG (red). To optimize viewing of this image, please see the online version of this article at www.kidney-international.org.

NELL-1 titers can be used for clinical follow-up needs to be confirmed in further studies.⁹

NELL-1-associated MN should be added to the list of serologically defined MN, including PLA2R- and THSD7A-associated MN. It is seen in older patients, has no sex predilection, has no IgG4 dominance, presents with nephrotic syndrome, and there is an absence of secondary

features such as malignancies (see below for discussion on malignancies in validation cohort), autoimmune disease, and infections. Interestingly, IgG subtyping performed in few cases of NELL-1-positive MN by IF and MS/MS showed that the predominant subclass was IgG1, whereas the predominant IgG subclass in PLA2R-positive MN is known to be IgG4. The kidney biopsy also shows no features that point to a secondary

Table 1 | Laboratory and kidney biopsy findings of NELL-1-associated MN

Case	Age	Sex	Urinary protein g/24 h ^a	Serum creatinine mg/dl ^b	Sclerosed/total glomeruli	IFTA	IF	EM
1 (MN5) ^c	65	M	1.5	1.7	1 scl/12	10	IgG 3+, C1q 1+, C3 2+	II
2	66	F	11	1.2	4 scl/13	10	IgG 3+, C3 1+	II
3	71	F	NA	4.0	6 scl/33	50	IgG 3+, IgA1+	II, seg
4	63	F	NA	1.1	5 scl/23	5	IgG 3+, C3 2+	II
5	66	F	NA	NA	1 scl/19	0	IgG 3+, C3 2+	I-II, seg
6	34	F	4.4	0.6	0 scl/26	0	IgG 3+, C3 1+	I-II
7	67	M	11.7	3	6 scl/20	10	IgG 3+, C3 2+	II
8	75	F	15	1.2	2 scl/8	10	IgG 3+, C3 2+	II
9	63	F	7.5	0.7	2 scl/28	10	IgG 3+, C3 3+	II, seg
10	61	F	9	1.2	5 scl/30	0	IgG 3+, C3 2+	II
11	63	M	12	1.6	12 scl/50	25	IgG 3+, C3 2+	II
12	51	F	7.1	0.6	2 scl/30	0	IgG 2+, C3 1+	I-II
13	63	F	4	1	0 scl/5	10	IgG 2+, C3 1+	I, seg
14	67	M	5	1.2	3 scl/11	10	IgG 3+, C3 2+	I-II
15	73	M	NA	2.5	3 scl/8	30	IgG 2+, C3 1+	I-II
16	75	F	3.7	0.8	2 scl/22	10	IgG 2+, C3 1+	II
17	68	F	7	0.9	0 scl/19	10	IgG 3+, C3 2+	I
18	65	M	6	1.0	3 scl/20	25	IgG 3+, C3 2+	II, seg
19	62	M	8.9	1.0	0 scl/1	Minimal cortex	IgG 3+, C3 2+	ND
20	55	F	4	0.6	1 scl/18	0	IgG 3+, C3 3+	I-II
21	82	M	NA	4.2	0 scl/9	20	IgG 3+, C3 3+	I
22	63	M	NA	3.2	9 scl/32	30	IgG 2+, C3 1+	II
23	56	M	NA	NA	22/38	40	IgG 3+, C3 1+	II
24	73	M	3	1.7	2 scl/22	0	IgG 3+, C3 1+	I-II
25	37	F	8	0.7	3 scl/61	0	IgG 3+, C3 1+	II, seg
26	60	M	3.1	1.2	0 scl/18	0	IgG 2+, C3 1+	I
27	66	M	NA	4.2	0 scl/5	0	IgG 3+, C3 1+	I
28	49	M	2.1	0.9	0 scl/17	0	IgG 2+, C3 1+	I
29	72	M	5	6.1	0 scl/1	0	IgG 2+, C3 2+	II
30 (MN1) ^c	78	M	4.5	1.7	4 scl/14	20	IgG 3+, C3 1+	II
31 (MN2) ^c	67	M	9.8	1.0	1 scl/18	0	IgG 3+, C3 3+	II
32 (MN3) ^c	71	F	12.0	0.4	1 scl/15	10	IgG 3+, C3 3+	I
33 (MN4) ^c	30	F	3.7	0.6	1 scl/11	<25	IgG 3+, C3 1+	ND
34	71	M	12.9	1.35	3 scl/16	<25	IgG 3+, C1q 1+ C3 3+	ND

C1q, complement component 1q; C3, complement component 3; EM, electron microscopy; IF, immunofluorescence microscopy (1–3+ represents intensity of scoring, scoring out of 3); IFTA, interstitial fibrosis and tubular atrophy; F, female; M, male; MN, membranous nephropathy; NA, not available; ND, not done; NELL-1, neural epidermal growth factor-like 1 protein; scl, sclerosed; seg, segmental EM grade I to IV.

^aMean urinary protein 7 ± 3.7 g/24 h.

^bMean serum creatinine 1.7 ± 1.3 mg/dl; cases 30, 31, 32, and 34 were associated with malignancies.

^cMN1 to MN5 represent the 5 cases in which serum was available and Western blot studies were performed (see Figure 5).

cause such as proliferative features on light microscopy, full house Ig staining including C1q on IF microscopy, and tubuloreticular inclusions in endothelial cells, and mesangial or subendothelial deposits on electron microscopy.

NELL-1 is a gene named after its similarity to a gene *Nel* that is strongly expressed in neural tissue encoding a protein with EGF-like repeats.¹⁰ *Nel* expression is present in all chick tissues, and the highest expression was in the brain. Nonneural tissues such as liver and kidney express very low levels of *Nel*.¹⁰ Since then, 2 genes homologous to *Nel*, *NELL-1*, and *NELL-2* have been identified.¹¹ The amino acid sequences of *NELL-1* and *NELL-2* are only about 50% homologous, suggesting that the 2 proteins are distinct with possibly different functions.¹² *NELL-1* encodes a 90-kDa secreted protein of 810 amino acids and contains conserved motifs including a secretory signal peptide, NH2-terminal thrombospondin-1 like molecule (TSPN), coiled-coil domain, 4 von Willebrand-type domains, and 6 EGF-like repeats (Figure 5c).¹³ The TSPN is the heparin binding domain and the EGF repeats are the protein kinase C

binding domains.¹⁴ *NELL-1* is highly expressed in osteoblasts and promotes bone regeneration. The C-terminal region of *NELL-1* mediates osteoblastic cell adhesion through integrin $\alpha 3 \beta 2$.^{15,16} *NELL-1* is overexpressed in patients with craniosynostosis, one of the common congenital craniofacial deformities, where it is specifically upregulated within prematurely fusing sutures.^{17,18} Mice overexpressing *NELL-1* also develop the craniosynostosis phenotype.¹⁹

In the kidney, *NELL-1* expression is higher in tubules while it is barely detectable in the glomeruli although 5% to 25% of glomerular cells express *NELL-1* at the mRNA level.^{11,20} However, when *NELL-1*-expressing human embryonic kidney cells were grown on gelatin-coated coverslips, *NELL-1* was deposited in the extracellular matrix after detachment of the cells, suggesting that *NELL-1* is likely present as an extracellular component and may be deposited in the GBM.¹⁵ Recently, it was shown *NELL-1* expression is down-regulated in areas of renal cell carcinoma while it is expressed in normal tubules and is thought to play an

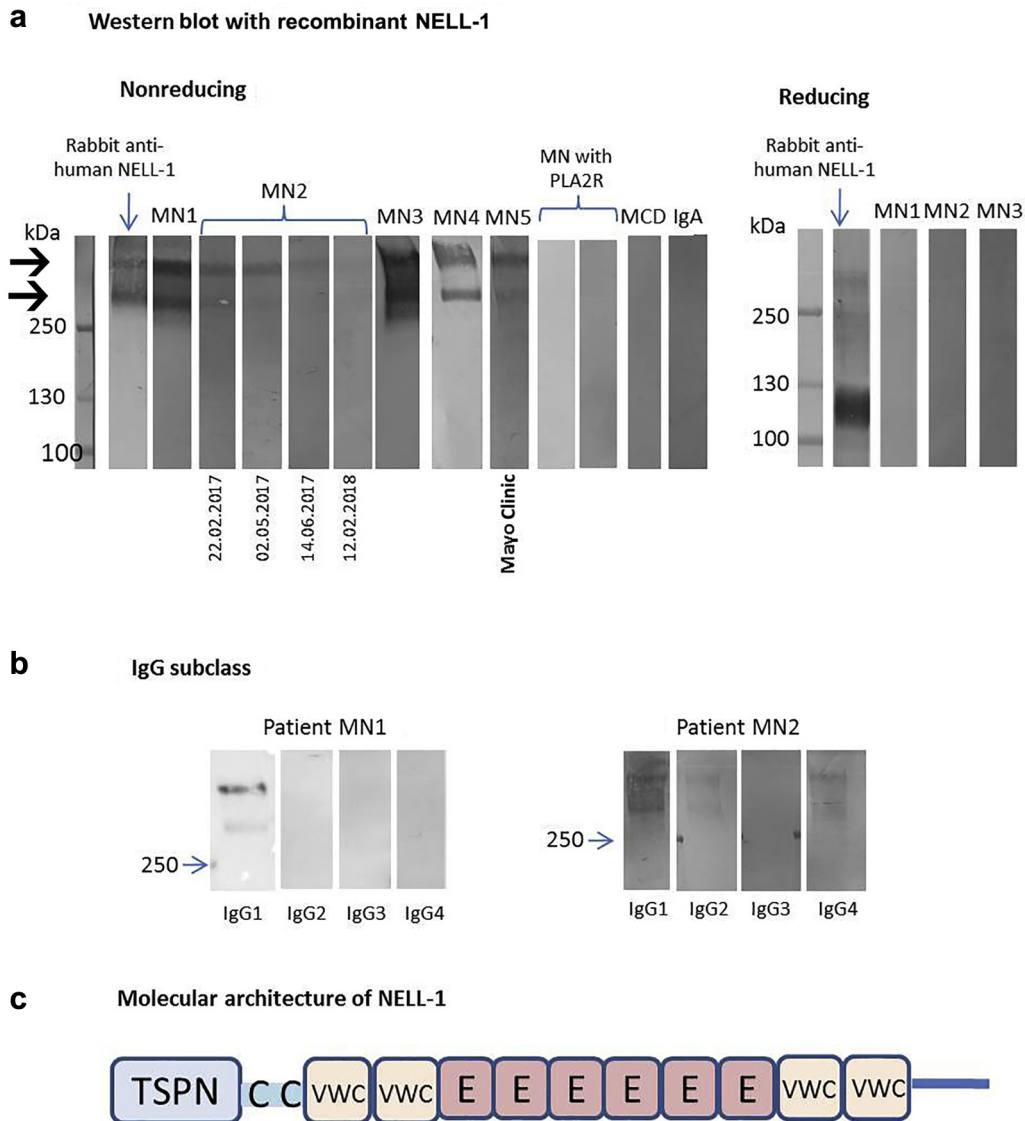


Figure 5 | Detection of anti-neural epidermal growth factor-like 1 protein (NELL-1) antibodies in the serum by Western blot analysis. (a) Western blotting shows reactivity of serum samples with recombinant human NELL-1 protein in 5 patients with NELL-1–associated membranous nephropathy (MN). Under nonreducing conditions, NELL-1 is detected predominantly as 280 kDa homodimers (bottom arrow) and 420 kDa homotrimers (top arrow) formed through a helical coiled-coil domain. In patient MN2, samples were available at the indicated time points; treatment with rituximab was started on June 14, 2017. Note the lack of reactivity of sera from patients with M-type phospholipase A2 receptor (PLA2R)–associated MN, with minimal change disease (MCD), and with IgA nephropathy. Under reducing conditions, NELL-1 resolves as monomeric bands of about 130 kDa, and reactivity of NELL-1–positive sera is lost, suggesting that the patient’s autoantibodies recognize conformation-dependent epitopes. (b) Western blotting shows that anti-NELL-1 autoantibodies are mainly carried by the IgG1 subclass in the first patient (MN1) while IgG2 and IgG4 subtypes were also present in the second patient. This pattern corresponds to the IgG subclass immunofluorescence pattern in biopsy. (c) The molecular architecture of NELL-1 is shown, and it includes an N-terminal TSP-1-like (TSPN), a coiled-coil (CC) domain, 4 von Willebrand factor type C (VWC) domains, and 6 epidermal growth factor–like domains (E).

important role in the renal cell carcinoma behavior.²¹ To the best of our knowledge, overexpression of NELL-1 has not been reported in any kidney disease. NELL-1–associated MN appears to be unique kidney disease associated with overexpression of NELL-1. As is the case for PLA2R and THSD7A,²² anti-NELL-1 antibodies recognize a conformation-dependent epitope (found both in 280-kDa homodimers and 420-kDa homotrimers formed through a helical coiled-coil domain). Further studies are needed to determine NELL-1 ultrastructural

localization at the podocyte and the potential role of anti-NELL-1 antibodies in podocyte adhesion and slit diaphragm stabilization.

Finally, a larger (23% of 126 cases) number of NELL-1–positive MN were detected in the pilot/discovery cohort cases at the Mayo Clinic compared with the smaller number of cases (5.9% of 84) from the French and Belgian validation cohorts. This may be due to genetic background differences as is seen in the variable geographic incidence of PLA2R- and

THSD7A-positive MN.²³ Thus, with regard to PLA2R, a retrospective study showed 89.6% prevalence of PLA2R-associated MN at the Tenon Hospital,²⁴ while there was a prevalence of only 48.1% among 592 biopsies of nonlupus MN at the Mayo Clinic (S. Sethi, 2019, unpublished data). Similarly, a recent study on THSD7A-associated MN reported a prevalence of 2.8% among the 1012 patients from 6 European cohorts,²⁵ while only 1 of 181 patients enrolled in Membranous Nephropathy Trial of Rituximab (MENTOR) study,²⁶ and 2 of 422 (<0.5%) patients screened at Mayo Clinic locations—Rochester, MN; Jacksonville, FL; and Phoenix, AZ—were found to be THSD7A positive (S. Sethi, 2019, unpublished data).

Interestingly, cancer was detected in 4 of 5 NELL-1-positive cases of the validation cohorts, while none of the 29 NELL-1 of the pilot and discovery Mayo Clinic cohort cases had cancer. The findings suggest that NELL-1-associated MN can occur in different settings including cancer as is also the case for PLA2R-associated MN. This also raises the question whether the small subset of NELL-1-positive MN associated with cancer can be truly classified as primary MN. Further studies are required to address this question.

Overall, 34 NELL-1-positive cases (16%) were identified in 210 PLA2R-negative biopsies with all cohorts combined, and that is more than double the number of THSD7A cases in the original study (15 of 154 PLA2R-negative, 10%).⁶ Taken together, the findings suggest that NELL-1 is the second most common antigen (after PLA2R) in primary MN. Further studies are needed to understand the prevalence discrepancy of NELL-1-positive MN.

In conclusion, we have identified a novel protein NELL-1 in a subset of PLA2R-negative MN in adult patients. NELL-1-associated MN appears to be a distinct type of primary MN.

METHODS

Patients and sample collection

Biopsies were received in the Renal Pathology Laboratory, Department of Laboratory Medicine and Pathology, Mayo Clinic, for diagnosis and interpretation between January 2015 and May 2018. Light microscopy, IF microscopy including PLA2R studies, and electron microscopy was performed in each case of MN. The clinical information was obtained from the accompanying charts. The study was approved by the Mayo Clinic Institutional Review Board. For control cases, we performed MS/MS on 111 cases that included 15 cases of time 0 kidney transplant biopsies, 17 cases of minimal change disease, 44 cases of focal segmental glomerulosclerosis, 7 cases of diabetic glomerulosclerosis, 5 cases of IgA nephropathy, and 23 cases of PLA2R-associated MN. For control IHC, we used 20 cases that included 4 cases of focal segmental glomerulosclerosis, 4 cases of IgA nephropathy, 4 cases of diabetes, and 8 cases of PLA2R-associated MN.

Validation cohorts

Two validation cohorts were used.

- (i) French cohort: Twenty-three unstained, blinded kidney biopsy slides of formalin-fixed paraffin-embedded (FFPE) tissue were

provided by the Institut national de la santé et de la recherche médicale (Inserm) UMR-S1155 (Tenon Hospital, Paris) and analyzed in the Pathology Research Core (Mayo Clinic) by IHC for NELL-1. All 23 cases were PLA2R- and THSD7A-negative MN. An additional 22 cases (FFPE) of PLA2R- and THSD7A-negative MN were stained for NELL-1 at Inserm UMR-S1155 using IF methodology.

- (ii) Belgian cohort: Thirty-nine unstained, blinded kidney biopsy slides of FFPE tissue of PLA2R- and THSD7A-negative MN were obtained in the UC Louvain Kidney Disease Network. These cases were stained for NELL-1 at Inserm UMR-S1155 using IF.

Protein identification by laser capture microdissection, trypsin digestion, nano-liquid chromatography Orbitrap MS/MS

For each case 10- μ m thick FFPE were obtained and mounted on a special polyethylene naphthalate membrane laser microdissection slide and using a Zeiss Palm Microbeam microscope (Carl Zeiss AG, Oberkochen, Germany), the glomeruli were microdissected to reach approximately 250,000 to 5000 μ m² per case. Resulting FFPE fragments were digested with trypsin and collected for MS/MS analysis. The trypsin-digested peptides were identified by nano-flow liquid chromatography electrospray tandem MS/MS using a Thermo Scientific Q-Exactive Mass Spectrometer (Thermo Fisher Scientific, Bremen, Germany) coupled to a Thermo Ultimate 3000 RSLCnano HPLC system. All MS/MS samples were analyzed using Mascot and X! Tandem set up to search a Swissprot human database. Scaffold (version 4.8.3, Proteome Software Inc., Portland, OR) was used to validate MS/MS-based peptide and protein identifications. Peptide identifications were accepted at >95.0% probability by the Scaffold Local FDR algorithm with protein identifications requiring a 2 peptide minimum and a 95% probability using Protein Prophet (Seattle, WA).²⁷ Details of laser capture and MS/MS are given in the [Supplementary Methods](#) and [Supplementary Table S2](#).

IHC, IF, and colocalization staining for NELL-1

Tissue sectioning and IHC staining were performed at the Pathology Research Core (Mayo Clinic, Rochester, MN) using the Leica Bond RX stainer (Leica Biosystems, Buffalo Grove, IL). FFPE tissues were sectioned at 5 μ m and IHC staining was performed online. Slides for the NELL-1 stain were retrieved for 20 minutes using Epitope Retrieval 2 (ethylenediamine tetraacetic acid; Leica Biosystems) and incubated in Protein Block (Dako) for 5 minutes. The NELL-1 primary antibody (Rabbit Polyclonal, Sigma #HPA051535) was diluted to 1:100 in Background Reducing Diluent (Dako; Agilent Technologies, Santa Clara, CA) and incubated for 15 minutes. The detection system used was Polymer Refine Detection System (Leica Biosystems). This system includes the hydrogen peroxidase block, post primary and polymer reagent, 3,3'-diaminobenzidine (DAB), and hematoxylin. Immunostaining visualization was achieved by incubating slides 10 minutes in DAB and DAB buffer (1:19 mixture) from the Bond Polymer Refine Detection System. To this point, slides were rinsed between steps with 1x Bond Wash Buffer (Leica Biosystems). Slides were counterstained for 5 minutes using Schmidt hematoxylin and molecular biology grade water (1:1 mixture), followed by several rinses in 1x Bond wash buffer and distilled water, this is not the hematoxylin provided with the Refine kit. Once the immunocytochemistry process was completed, slides were removed from the stainer and rinsed in tap water for 5 minutes. Slides were dehydrated in increasing concentrations of ethyl alcohol

and cleared in 3 changes of xylene prior to permanent cover slipping in xylene-based medium.

IF staining was performed on FFPE sections retrieved for 30 minutes using target retrieval solution high pH (Dako) in pressure cooker equipment (Bio SB, Santa Barbara, CA). The NELL-1 primary antibody (rabbit polyclonal, Atlas antibodies) was diluted to 1:100 in blocking solution (2% calf fetal serum and 2% normal goat serum) and incubated overnight at 4 °C with retrieved biopsy sections. Next, the slides were incubated with secondary antibody goat Alexa 488-conjugated anti-rabbit Fab IgG (Life Technologies, Thermo Fisher Scientific, Waltham, MA). Anti-human IgG Alexa Fluor 647 rabbit monoclonal antibody (Sigma-Aldrich, St. Louis, MO) was then reacted with the retrieved tissue as described above. Finally slides were mounted in mounted medium (Thermo Fisher Scientific) and covered with LDS2460EP cover glass slides. Colocalization of NELL-1 and IgG along the glomerular basement membrane was examined by confocal microscopy using a Leica TCS-SP2 and analyzed with Leica Confocal Software (version 2.61; Leica, Wetzlar, Germany).

Western blot analysis

The protein sample, recombinant human NELL-1 (R&D Systems, Minneapolis, MN) was diluted with nonreducing or reducing Laemmli sample buffer (Bio-Rad Laboratories, Hercules, CA) and boiled for 5 minutes. Samples were loaded into Criterion 4% to 15% TGX gels (Bio-Rad) and electrophoresed in Tris-glycine-sodium dodecylsulfate running buffer. Proteins were transferred to poly (vinylidene difluoride) membranes according to standard protocols and the membranes were blocked with Pierce Protein-Free Blocking buffer (Thermo Fisher Scientific). Membranes were incubated overnight at 4 °C with sera from patients, controls (dilution 1:50), and rabbit polyclonal antibodies (dilution 1:500) against NELL-1 (Abcam, Cambridge, UK). Subsequently, blots were washed and incubated for 2 hours at room temperature with goat-anti human or goat anti-rabbit IgG, alkaline phosphatase conjugate (Sigma-Aldrich). Immunoreactive proteins were visualized with 5-bromo-4-chloro-3-indolyl phosphate/nitro blue tetrazolium liquid substrate system (Sigma-Aldrich).

For subclass detection in nonreducing conditions, blots were incubated with mouse monoclonal anti-human IgG subclass antibodies (SouthernBiotech, Birmingham, AL), then revealed with alkaline phosphatase-conjugated polyclonal anti-mouse IgG antibody (Vector Labs, Burlingame, CA).

DISCLOSURE

All the authors declared no competing interests.

ACKNOWLEDGMENTS

We would like to thank the Mayo Clinic, Proteomics Core (a shared resource of the Mayo Clinic Cancer Center [National Cancer Institute {NCI} P30 CA15083]); Department of Laboratory Medicine and Pathology and the Pathology Research Core, Mayo Clinic; and the Fulk Family Foundation. PR received the following: European Research Council ERC-2012-ADG_20120314 grant no. 322947, 7th Framework Programme of the European Community contract no. 2012-305608 (European Consortium for High-Throughput Research in Rare Kidney Diseases), and the National Research Agency grant MNaims (ANR-17-CE17-0012-01). We are greatly indebted to the clinicians who took care of the patients in the Department of Nephrology and Dialysis at Tenon Hospital, Paris, over the last 20 years; to Isabelle Brocheriou (MD, PhD) from the Department of Pathology, Pitié Salpêtrière Hospital, Paris; and to Nadhir Yousfi (PhD) for help in Western blotting experiments. We would like to thank

Romain Morichon (PhD), Confocal Microscopy Platform, Saint-Antoine Hospital, Paris; Eva Compérat; and all staff members of the Tenon Hospital Biological Resource Center (BRC CANCER HUEP- Paris) for their help in centralizing and managing biological data collection. We also thank the clinicians from the UC Louvain Kidney Disease Network for patients' referral; Selda Aydin (MD, PhD) from the Department of Pathology of the Cliniques universitaires Saint-Luc, Brussels, for pathological diagnosis; and Nicolas Hanset (MD) for data collection.

AUTHOR CONTRIBUTIONS

SS and FCF designed the study. SS wrote the manuscript, interpreted the kidney biopsy, clinical, IHC and MS data. BM and CC performed the laser microdissection and MS. AR helped in gathering clinical data. LG performed the IHC. PR, DB, and HD provided tissue for the validation cohort and also performed the confocal studies and Western blot analysis. JM and MJ provided clinical information and tissue for the Belgian validation cohort. The manuscript was drafted and written by SS, with input as appropriate from the rest of the investigators.

SUPPLEMENTARY MATERIAL

[Supplementary File \(PDF\)](#)

Supplementary Methods. Details of laser microdissection and mass spectrometry.

Figure S1. An example of MS/MS spectra match to a sequence from NELL-1.

Figure S2. Electron microscopy showing segmental subepithelial electron-dense deposits in 6 cases.

Figure S3. Immunohistochemical staining for NELL-1 in NELL-1-positive MN cases.

Figure S4. Confocal microscopy of additional NELL-1-positive MN case.

Table S1. Glomerular area dissected per case.

REFERENCES

- Beck LH Jr, Salant DJ. Membranous nephropathy: from models to man. *J Clin Invest.* 2014;124:2307–2314.
- Ronco P, Debiec H. Pathophysiological advances in membranous nephropathy: time for a shift in patient's care. *Lancet.* 2015;385:1983–1992.
- Couser WG. Primary membranous nephropathy. *Clin J Am Soc Nephrol.* 2017;12:983–997.
- Beck LH Jr, Bonegio RG, Lambeau G, et al. M-type phospholipase A2 receptor as target antigen in idiopathic membranous nephropathy. *N Engl J Med.* 2009;361:11–21.
- Tomas NM, Hoxha E, Reinicke AT, et al. Autoantibodies against thrombospondin type 1 domain-containing 7A induce membranous nephropathy. *J Clin Invest.* 2016;126:2519–2532.
- Tomas NM, Beck LH, Meyer-Schwesinger C, et al. Thrombospondin type-1 domain-containing 7A in idiopathic membranous nephropathy. *N Engl J Med.* 2014;371:2277–2287.
- Sethi S, Madden BJ, Debiec H, et al. Exostosin 1/exostosin 2-associated membranous nephropathy. *J Am Soc Nephrol.* 2019;30:1123–1136.
- Beck LH, Fervenza FC, Beck DM, et al. Rituximab-induced depletion of anti-PLA2R autoantibodies predicts response in membranous nephropathy. *J Am Soc Nephrol.* 2011;22:1543–1550.
- De Vriese AS, Glasscock RJ, Nath KA, et al. A proposal for a serology-based approach to membranous nephropathy. *J Am Soc Nephrol.* 2017;28:421–430.
- Matshuhashi S, Noji S, Koyama E, et al. New gene, nel, encoding a Mr 93 K protein with EGF-like repeats is strongly expressed in neural tissues of early stage chick embryos. *Dev Dyn.* 1995;203:212–222.
- Watanabe TK, Katagiri T, Suzuki M, et al. Cloning and characterization of two novel human cDNAs (NELL1 and NELL2) encoding proteins with six EGF-like repeats. *Genomics.* 1996;38:273–276.
- Luce MJ, Burrows PD. The neuronal EGF-related genes NELL1 and NELL2 are expressed in hemopoietic cells and developmentally regulated in the B lineage. *Gene.* 1999;231:121–126.

13. Zhang X, Zara J, Siu RK, et al. The role of NELL-1, a growth factor associated with craniosynostosis, in promoting bone regeneration. *J Dent Res*. 2010;89:865–878.
14. Kuroda S, Oyasu M, Kawakami M, et al. Biochemical characterization and expression analysis of neural thrombospondin-1-like proteins NELL1 and NELL2. *Biochem Biophys Res Commun*. 1999;265:79–86.
15. Hasebe A, Tashima H, Ide T, et al. Efficient production and characterization of recombinant human NELL1 protein in human embryonic kidney 293-F cells. *Mol Biotechnol*. 2012;51:58–66.
16. Hasebe A, Nakamura Y, Tashima H, et al. The C-terminal region of NELL1 mediates osteoblastic cell adhesion through integrin $\alpha 3\beta 1$. *FEBS Lett*. 2012;586:2500–2506.
17. Ting K, Vastardis H, Mulliken JB, et al. Human NELL-1 expressed in unilateral coronal synostosis. *J Bone Miner Res*. 1999;14:80–89.
18. Zhang X, Carpenter D, Bokui N, et al. Overexpression of Nell-1, a craniosynostosis-associated gene, induces apoptosis in osteoblasts during craniofacial development. *J Bone Miner Res*. 2003;18:2126–2134.
19. Zhang X, Kuroda S, Carpenter D, et al. Craniosynostosis in transgenic mice overexpressing Nell-1. *J Clin Invest*. 2002;110:861–870.
20. The Human Protein Atlas. NELL1. Available at: www.proteinatlas.org/ENSG00000165973-NELL1/tissue/kidney. Accessed August 25, 2019.
21. Nakamura R, Oyama T, Tajiri R, et al. Expression and regulatory effects on cancer cell behavior of NELL1 and NELL2 in human renal cell carcinoma. *Cancer Sci*. 2015;106:656–664.
22. Herwig J, Skuza S, Sachs W, et al. Thrombospondin type 1 domain-containing 7A localizes to the slit diaphragm and stabilizes membrane dynamics of fully differentiated podocytes. *J Am Soc Nephrol*. 2019;30:824.
23. Hihara K, Iyoda M, Tachibana S, et al. Anti-phospholipase A2 receptor (PLA2R) antibody and glomerular PLA2R expression in Japanese patients with membranous nephropathy. *PLoS One*. 2016;11:e0158154.
24. Pourcine F, Dahan K, Mihout F, et al. Prognostic value of PLA2R autoimmunity detected by measurement of anti-PLA2R antibodies combined with detection of PLA2R antigen in membranous nephropathy: a single-centre study over 14 years. *PLoS One*. 2017;12:e0173201.
25. Zaghriani C, Seitz-Polski B, Justino J, et al. Novel ELISA for thrombospondin type 1 domain-containing 7A autoantibodies in membranous nephropathy. *Kidney Int*. 2019;95:666–679.
26. Fervenza FC, Appel GB, Barbour SJ, et al. Rituximab or cyclosporine in the treatment of membranous nephropathy. *N Engl J Med*. 2019;381:36–46.
27. Nesvizhskii A, Keller A, Kolker E, et al. A statistical model for identifying proteins by tandem mass spectrometry. *Anal Chem*. 2003;75:4646–4658.